Nanoscale

RSC Publishing

PAPER

View Article Online
View Journal | View Issue

Cite this: *Nanoscale*, 2013, **5**, 8242

Exploring and exploiting the synergy of non-covalent interactions on the surface of gold nanoparticles for fluorescent turn-on sensing of bacterial lipopolysaccharide†

Jinhong Gao, Yangwei Lai, Chuanliu Wu* and Yibing Zhao*

Received 14th May 2013
Accepted 25th June 2013

DOI: 10.1039/c3nr02490c

www.rsc.org/nanoscale

The sensing of lipopolysaccharide (LPS) relies on the synergy of multiple electrostatic and hydrophobic interactions between LPS and the sensor. However, how non-covalent interactions are coordinated to impel the recognition process still remains elusive, and the exploration of which would promote the development of LPS sensors with higher specificity and sensitivity. In this work, we hypothesize that Au NPs would provide a straightforward and flexible platform for studying the synergy of non-covalent interactions. The detailed mechanism of interactions between the designed fluorescent probes and Au NPs with two distinct surface properties was systematically explored. We demonstrated that only when the electrostatic attraction and hydrophobic stacking are both present, the binding of fluorescent probes onto Au NPs can be not only highly efficient, but also positively cooperative. After that, hybrid systems that consist of Au NPs and surface-assembled fluorescent probes were exploited for fluorescent turn-on sensing of LPS. The results show that the sensitivity and selectivity to LPS relies strongly on the binding affinity between fluorescent probes and Au NPs. Fluorescent probes assembled Au NPs thus provide an attractive platform for further optimization of the sensitivity/selectivity of LPS sensing.

Introduction

Lipopolysaccharide (LPS), also known as lipoglycan or endotoxin, is a major component in the outer membranes of Gram-negative bacteria, which contributes greatly to the structural integrity of the bacteria.[1] The release of LPS from bacteria can elicit strong immune responses in humans, while at higher concentration it may also lead to septic shock, organ failure, and even death.[2] Due to its high toxicity, a variety of chemical sensors have been developed for the specific and sensitive determination of LPS. To date, only one sensing system is clinically used for LPS determination, which exploits the gel formation of limulus amebocyte lysate (LAL) in the presence of LPS.[3] However, this assay suffers from poor reproducibility and quantitative ability, as well as potential interference from other carbohydrate derivatives, such as β-glucans. Other sensors that exploit synthetic receptors, to some extent, overcome the shortcomings of LAL assay, which however possess limitations in either sensitivity or selectivity.[4] Very recently, many studies have been dedicated to the development of fluorescent turn-on sensors,[5] a kind of sensor which is very suitable for the determination of LPS with a high sensitivity. Despite the very innovative aspects of these studies, the construction of fluorescent turn-on sensors usually involves very sophisticated organic synthesis and/or implementation of experiential knowledge regarding the complicated interactions between LPS and the designed sensors.

Molecular recognition, especially for the recognition of large molecules, usually relies on the synergy of non-covalent interactions including electrostatic and hydrophobic interactions, van der Waals forces, and hydrogen bonds.[6] LPS consists of a lipid and a polysaccharide joined by an oligosaccharide unit, in which the oligosaccharide and lipid units render LPS negatively charged amphiphilicity, a property that provides the basis for LPS recognition. For example, a fluorescent polymer that has recently been reported shows very high selectivity and sensitivity to LPS owing to multiple electrostatic and hydrophobic cooperative interactions between LPS and the sensor.[5] However, to what extent and how these non-covalent interactions are coordinated to impel the recognition process still remains elusive, and the exploration of which would not only promote the development of LPS sensors with higher specificity and sensitivity, but also provide directions to the rational design of sensing systems for other large molecules.

Department of Chemistry, College of Chemistry and Chemical Engineering and the MOE Key Laboratory of Analytical Sciences, Xiamen University, Xiamen, 361005, P.R. China. E-mail: chlwu@xmu.edu.cn; ybzhao@xmu.edu.cn; Fax: +86 592 2183206; Tel: +86 592 2183206

† Electronic supplementary information (ESI) available: ^{1}H-NMR characterization of **2–4**; introduction of the Hill equation; additional figures. See DOI: 10.1039/c3nr02490c

Non-covalent interactions also exist in various biomaterials–biology interfaces, which play vital roles in defining the destination of biomaterials in biological systems.[7] In addition, recently there has been an increased interest in exploiting the non-covalent interactions on the surface of nano-materials (*e.g.* gold nanoparticles – Au NPs) for the construction of hybrid materials such as catalysts, sensors, and drug delivery systems.[8] In this context, Au NPs with a well-defined surface monolayer have been synthesized to probe how their "intrinsic" surfaces affect the interactions of nano-materials with living organisms and/or molecules in environments. For instance, Moyano *et al.* have recently reported the use of engineered Au NPs to determine the sole effect of surface hydrophobicity on the immune response of splenocytes.[9] Besides, owing to their easiness of surface engineering and appealing optical properties, Au NPs have emerged as attractive scaffolds for numerous applications such as sensing, catalysis, and recognition.[10]

We hypothesize that Au NPs would provide a straightforward and flexible platform for studying the synergy of surface non-covalent interactions, an exploration which would greatly benefit the use of Au NPs for sensing and recognition, in which multiple electrostatic and hydrophobic cooperative interactions may be involved. In this work, we systematically explored the non-covalent interactions between guest molecules (*i.e.*, fluorescent probes) and Au NPs with two different surfaces (Scheme 1). Fluorescent probes with different hydrophobicity were designed and prepared through conjugating the fluorophore with alkyl chains of different length. We demonstrated that only when electrostatic attraction and hydrophobic stacking are both present, the binding of fluorescent probes onto the surface of Au NPs can be not only highly efficient, but also positively cooperative. After that, sensing systems that comprise of Au NPs and different surface-assembled fluorescent probes were developed and used for fluorescent turn-on sensing of LPS.

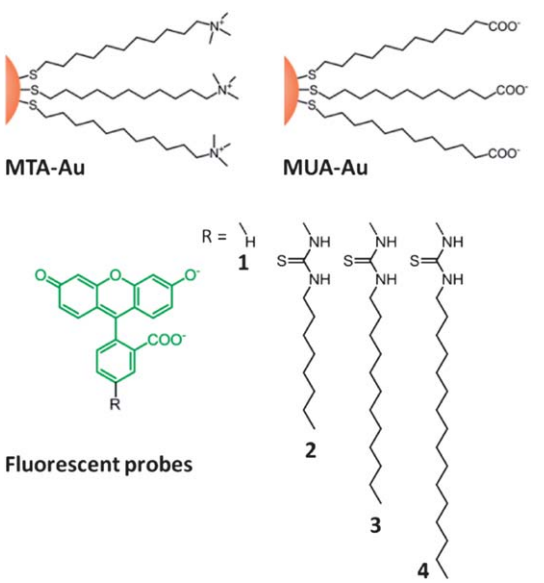

Scheme 1 Chemical structures of the MTA-Au and MUA-Au, and anionic fluorescent probes (guest molecules, **1–4**).

Experimental section

Materials and methods

All chemicals were purchased from major suppliers such as Alfa Aesar (Tianjin), Sigma-Aldrich (Beijing), Sangon (Shanghai), J&K (Guangzhou), and used as received. All UV-Vis absorption and fluorescence spectra were recorded using a U-3900H spectrophotometer (Hitachi) and a F-7000 fluorescence spectrophotometer (Hitachi). The transmission electron microscope (TEM) images were taken on a JEOL JEM-2000EX microscope. ^{1}H NMR spectra were collected on a Bruker Advance-400 spectrometer. Electrospray ionization mass spectroscopy (ESI-MS) was carried out on a Bruker Esquire 3000 plus mass spectrometer. Millipore ultrapure water was used throughout the experiments.

Preparation of Au NPs

Au NPs were prepared by sodium citrate-mediated reduction of $HAuCl_4$.[11] 100 mL of $HAuCl_4$ aqueous solution (41 mg, 1 mM) was heated to reflux under stirring, to which 10 mL of sodium citrate aqueous solution (38.8 mM) was added rapidly. The solution was heated under reflux with vigorous stirring for 25 min, leading to a gradual change of the color from pale yellow to wine red. After that, the solution was cooled to room temperature with slow and constant stirring. The resulting solution of Au NPs was characterized by an absorption maximum at 520 nm. The size of the prepared Au NPs was about 13 nm (from TEM images). It was reported that the extinction coefficient of 13 nm Au NPs at 520 nm is around 2.7×10^8 M^{-1} cm^{-1}.[12]

Preparation of monolayer protected Au NPs

MTA-Au and MUA-Au (Au NPs functionalized with a monolayer of (11-mercapto-undecyl)-trimethylammonium (MTA) and 11-mercaptoundecanoic acid (MUA), respectively) were prepared by a reported ligand-exchange approach.[13] For the preparation of MTA-Au, 150 μL of MTA aqueous solution (10 mM) was added rapidly into 10 mL of the as-prepared Au NPs under moderate stirring. To this mixture, 30 μL of 1 M aqueous HCl was then added. The solution was kept at room temperature for 3 hours. Subsequently, the obtained MTA protected Au NPs were purified by centrifugation (11 800 rpm, 20 min) and decantation several times, and washed with water to remove the unbound MTA and detached sodium citrate. MTA-Au was finally dispersed in water for further use. The concentration of MTA-Au can be determined by using a UV-Vis spectrophotometer. The procedures were modified slightly for the preparation of MUA-Au. Before the addition of MUA ligand, the pH of the as-prepared Au NPs solution was tuned to 9.0 by adding a proper amount of 1 M aqueous NaOH. Then, 150 μL of MUA solution in methanol (10 mM) was added. After 3 hours, the resulting MUA-Au was purified as described previously for the purification of MTA-Au.

Synthesis of fluorescent probes (2–4)

Fluorescent probes (**2–4**) were synthesized by conjugating fluorescein isothiocyanate (FITC) with hydrophobic alkyl chains of different length (*i.e.* octylamine, ODA; dodecylamine, DDA; hexadecylamine, HDA).[14] Typically, 4 mg ODA (or 5.7 mg DDA, 7

mg HDA) was reacted with 20 mg FITC in 50 mL dimethylformamide (DMF) at 50 °C for 48 hours. After that, 25 mL water was added into the solution to precipitate ODA–FITC (**2**) conjugate (or DDA–FITC, **3**; HDA–FITC, **4**). The obtained precipitate (**2–4**) was then filtered out, washed twice with water, dried, and stored in the dark for further use. The obtained compounds were characterized by ^{1}H NMR and ESI-MS: **2**, ^{1}H NMR (400 MHz, DMSO): δ 10.10 (s, 2H), 9.90 (s, 1H), 8.24 (s, 1H), 8.10 (s, 1H), 7.74 (s, 1H), 7.17 (d, J = 8.3 Hz, 2H), 6.67 (s, 2H), 6.64–6.54 (m, 3H), 1.56 (dd, J = 13.3, 6.6 Hz, 2H), 1.27 (d, J = 25.9 Hz, 12H), 0.85 (t, J = 6.8 Hz, 3H). ESI-MS: m/z, $(M + H)^+$, calculated: 519.62; found: 519.5. **3**, ^{1}H NMR (400 MHz, DMSO): δ 10.10 (s, 2H), 9.90 (s, 1H), 8.24 (s, 1H), 8.10 (s, 1H), 7.74 (s, 1H), 7.17 (d, J = 8.3 Hz, 2H), 6.67 (s, 2H), 6.64–6.54 (m, 3H), 1.56 (dd, J = 13.3, 6.6 Hz, 2H), 1.27 (d, J = 25.9 Hz, 20H), 0.85 (t, J = 6.8 Hz, 3H). ESI-MS: m/z, $(M + H)^+$, calculated: 575.25; found: 575.1. **4**, ^{1}H NMR (400 MHz, DMSO): δ 10.10 (s, 2H), 9.90 (s, 1H), 8.24 (s, 1H), 8.10 (s, 1H), 7.74 (s, 1H), 7.17 (d, J = 8.3 Hz, 2H), 6.67 (s, 2H), 6.64–6.54 (m, 3H), 1.56 (dd, J = 13.3, 6.6 Hz, 2H), 1.27 (d, J = 25.9 Hz, 28H), 0.85 (t, J = 6.8 Hz, 3H). ESI-MS: m/z, $(M + H)^+$, calculated: 631.84; found: 631.5.

Binding of 1–4 onto the surface of MTA-Au and MUA-Au

The binding experiments were performed in 10 mM 4-(2-hydroxyethyl)-1-piperazineethanesulfonic acid (HEPES) buffer (pH 7.0, 20% ethanol) at room temperature. All reagents (**1–4** and Au NPs) were prepared in 10 mM HEPES buffer (pH 7.0, 20% ethanol). Typically, to a solution containing 0.1 mL of 500 nM **1** (or **2**, **3**, **4**), different amounts of Au NPs (2.2 nM) was added, and the volume of the solution was adjusted to 1.0 mL by adding HEPES buffer (10 mM, pH 7.0, 20% ethanol) to achieve a final concentration of 50 nM for **1**, **2**, **3** or **4**. After 20 min, the fluorescence spectra of the solutions were recorded using a fluorescence spectrophotometer.

Fluorescent turn-on sensing of LPS

All reagents (**2–4**, Au NPs and LPS) were first dissolved in 10 mM HEPES buffer (pH 7.0, 20% ethanol). To a tube containing 100 μL of 0.5 μM probes (**3** or **4**) solution and 40 μL of MTA-Au solution (2.2 nM), 0.76 mL HEPES buffer was added. The solution was mixed thoroughly and kept at room temperature for 10 min, which leads to the formation of a **3**–MTA-Au (or **4**–MTA-Au) supramolecular complex. For the preparation of the **2**–MTA-Au complex, 70 μL of MTA-Au solution (2.2 nM) was added instead due to its relatively low quenching efficiency for the fluorescence of probe **2**. Subsequently, different volumes of LPS (10 μM) solution were added, and the volume of the mixture solution was adjusted to 1.0 mL by adding HEPES buffer. After 20 min, the fluorescence spectra of the reaction solution were recorded using a fluorescence spectrophotometer.

Results and discussion

Binding of 1–4 to MTA-Au

Au NPs functionalized with a monolayer of MTA (MTA-Au) were prepared by published methods (Fig. S1†).[13] The obtained MTA-Au was characterized by UV-Vis absorption spectroscopy, dynamic light scattering (DLS) and zeta-potential measurement. We found that the surface MTA monolayer renders Au NPs not only good stability in aqueous solutions, but also a positively charged amphiphilic surface (Fig. S2†) which represents a model scaffold for interacting with guest molecules *via* electrostatic and hydrophobic forces. Anionic fluorescent probes (guest molecules, **1–4**) with different hydrophobicity were synthesized by conjugating fluorescein (**1**) with alkyl chains of different length (Scheme 1). Au NPs are efficient fluorescent quenchers, allowing their interactions with the probes to be followed by fluorescence spectroscopy. Fig. 1 shows the change of fluorescent intensity of **1–4** as the concentration of MTA-Au increased in HEPES buffer (10 mM, pH 7.0, 20% ethanol). We found that the fluorescence of probes with alkyl chains (**2–4**) can be quenched markedly by the addition of MTA-Au, while the fluorescence of **1** remains relatively stable. A noticeable effect of alkyl chain length on the fluorescent quenching efficiency was also observed. These findings suggest that the hydrophobic interaction between **2–4** and MTA-Au should be the predominant driving force responsible for the binding of fluorescent probes on the surface of MTA-Au, while the effect of the electrostatic attraction was less important.

The binding constants K_d of **1–4** for MTA-Au were then extracted from the fluorescent quenching by a linear regression of the curves in Fig. 2a through the Hill equation (ESI†),[15] which was found to be increased from 1.393×10^9 mol^{-1} L (**1**) to 1.681×10^{10} mol^{-1} L (**2**), 3.263×10^{10} mol^{-1} L (**3**) and 4.469×10^{10} mol^{-1} L (**4**) as the length of alkyl chains increased (Fig. 2b). Deviations from the linear correlation may indicate greater complexity not taken into account in the quantitative model. It is very likely that the inevitable self-quenching between the bound fluorescent probes on the surface of Au NPs also contributes to the observed extent of fluorescent quenching, which may also lead to deviations from the expected linear trend. We further examined the binding cooperativity for **1–4** onto MTA-Au by comparing their Hill coefficient n, a value which was obtained from the slope of the plots in Fig. 2a. Interestingly, the Hill coefficient n increased from 1.13 (**1**) to

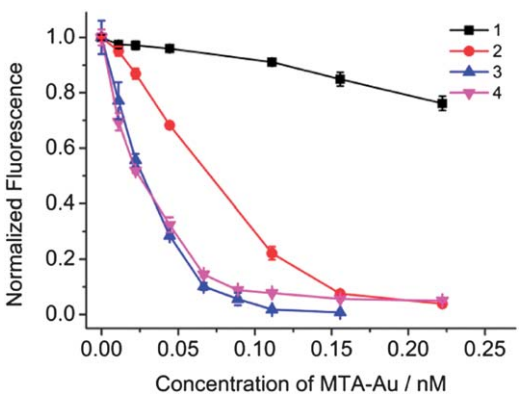

Fig. 1 Fluorescence response of fluorescent probes (**1–4**) upon the addition of MTA-Au in HEPES buffer (10 mM, pH 7.0, 20% ethanol). Data are presented as mean ± SD (n = 3).

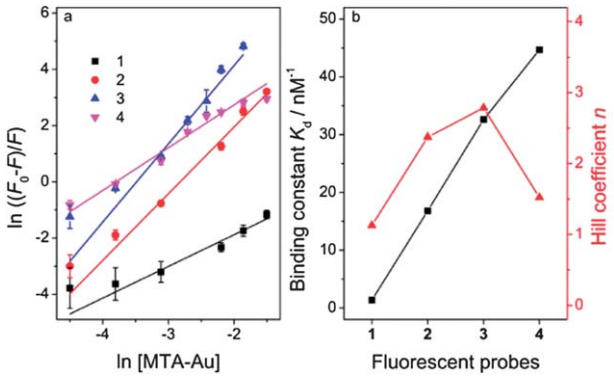

Fig. 2 (a) Fluorescence quenching data of **1–4** by MTA-Au, which were fitted by the Hill equation (solid line); data are presented as mean ± SD ($n = 3$); (b) binding constant K_d (black) of **1–4** for MTA-Au and Hill coefficient n (red) extracted from the linear regression of data in (2a).

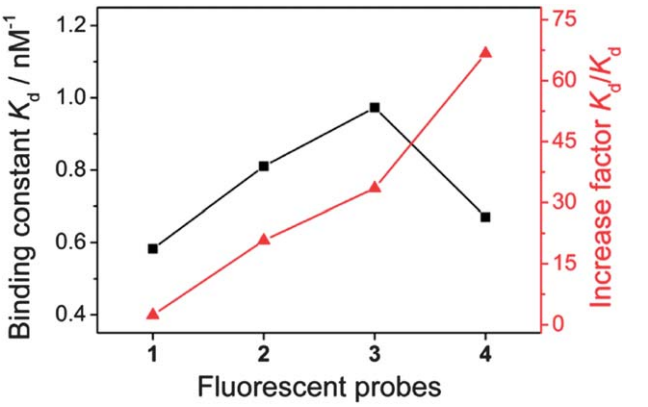

Fig. 3 Binding constants K (black) of **1–4** for MUA-Au extracted from fluorescence quenching data and the increase factor K_d/K_d (red) represents the difference between the binding constants of **1–4** for MTA-Au and that for MUA-Au.

2.37 (**2**) and 2.79 (**3**), and then decreased to 1.52 (**4**), reflecting a very complex and different cooperative binding process for each probe (Fig. 2b). For **2–4**, we observed positively cooperative binding ($n > 1$), which indicates that their binding strength to MTA-Au becomes progressively stronger as more probe molecules bind. In contrast, the affinity of **1** for MTA-Au is somewhat independent of the bound probe molecules ($n \approx 1$). The observed high-cooperativity of binding (**2** and **3**) should arise from the synergistic enhancement of intermolecular hydrophobic interactions between probe molecules, which leads to ordered stacking of **2** or **3** on the surface of Au NPs due to the perfect matching in length between alkyl chains of the probe molecules and that of MTA monolayer, while a lengthy alkyl chain leads to diminished cooperative binding for **4**, which indicates a relative disordered stacking of **4** on the surface of Au NPs. These findings have strong implications considering the effect of binding cooperativity when exploring or exploiting non-covalent interactions on the surface of nanoparticles.

Binding of 1–4 to MUA-Au

In the next step, Au NPs with a negatively charged amphiphilic surface (MUA-Au) were prepared by functionalizing Au NPs with a monolayer of MUA. The binding constants K_d of **1–4** for MUA-Au were then measured and compared with that for MTA-Au in order to examine the effect of electrostatic attraction/repulsion on the interactions between **1–4** and the surface of Au NPs. It was surprising to observe that the binding constants of **1–4** for MUA-Au (Fig. 3) or their efficiency of fluorescent quenching (Fig. S6†) were extremely lower than that for MTA-Au, which strongly implies that not only the hydrophobic interaction, but also the electrostatic attraction/repulsion plays a vital role in the interaction of **1–4** with Au NPs. This may also raise a query on a preceding deduction that the effect of the electrostatic attraction on the binding of **1–4** onto MTA-Au was less important. A further quantitative comparison shows that the binding constants of **1–3** for MUA-Au increased slightly as the length of alkyl chains increased, a result which is, to some extent, consistent with that observed in MTA-Au, reflecting a contribution of the hydrophobic interaction on the binding events. However, a lengthy alkyl chain (**4**) results in diminished binding to the MUA-Au likely due to the mismatch of the length of alkyl chain in probe molecules and MUA monolayer, a limitation which may hamper the hydrophobic binding of **4** onto MUA-Au. In addition, the binding cooperativity of **1–4** for MUA-Au was found to be in the range of 0.79–1.11 (Fig. S7†), which represents an anti-cooperative ($n < 1$) or non-cooperative ($n \approx 1$) binding model. This result was in great contrast with that obtained from the binding of **1–4** to MTA-Au, which directly demonstrates the effect of the electrostatic attraction between **1–4** and the surface of MTA-Au on the observed positively cooperative binding process. Moreover, Fig. 3 shows that the difference between the binding constants of **1–4** for MTA-Au and that for MUA-Au was significantly more pronounced (from 2.8-fold difference for **1** to 66.7-fold difference for **4**) as the length of the alkyl chain of fluorescent probes increased. This indicates, in combination with the preceding data, that the importance of the interplay/synergy of the electrostatic attraction and hydrophobic interaction on the binding of fluorescent probes onto Au NPs. Therefore, it is conceivable to conclude that only when both the electrostatic attraction and hydrophobic stacking are present, the binding of fluorescent probes onto Au NPs can be not only highly efficient, but also positively cooperative.

LPS sensing

Supramolecular systems that consist of Au NPs and surface-assembled fluorescent probes have been attractive scaffolds for the construction of fluorescent turn-on sensors.[16] The principle of this kind of sensing is to exploit the reversibility of non-covalent binding of fluorescent probes onto Au NPs, a property which can be quantitatively associated with fluorescent signal response.[17] We then explored the feasibility of using our supramolecular systems (*i.e.* surface **2–4** assembled MTA-Au) for LPS sensing. It was found that the fluorescence of **2–4** can be quenched almost completely when the concentration of MTA-Au is higher than 0.2 nM (Fig. 1). This means that one particle is capable of binding more than 250 fluorescent probe molecules.

Three sensors that are **2**–MTA-Au, **3**–MTA-Au, and **4**–MTA-Au, which respectively exploit the binding of **2**, **3**, and **4** onto the surface of MTA-Au were prepared by mixing proper amounts of MTA-Au and **2–4** in HEPES buffer (10 mM, pH 7.0, 20% ethanol). The fluorescence of **2–4** was quenched rapidly and significantly as expected. After that, LPS of different concentrations was added into the above mixtures, which resulted in a rapid (Fig. S8†) and concentration-dependent (Fig. 4) recovery of fluorescence.

LPS contains at least six fatty acid chains and many negative charges, which render LPS a high affinity to the surface of MTA-Au. It is not surprising that the binding of LPS onto the surface of MTA-Au can effectively displace the surface bound fluorescent probes, thus leading to a rapid and sensitive fluorescence response. In Fig. 4, we observed that the fluorescence of the sensing systems can be gradually restored to approximately 30–50% of their original values upon addition of LPS from 0 to 1.0 μM. The relative lower extent of fluorescence recovery for **2**–MTA-Au (~30%) likely resulted from the increased amount of MTA-Au that was added strategically for further quenching of **2**. In addition, the addition of LPS led to a 7-, 22-, and 8-fold increase of fluorescence intensity for **2**–MTA-Au, **3**–MTA-Au, and **4**–MTA-Au, respectively. The de-quenching effect observed for **2**–MTA-Au or **4**–MTA-Au was significantly less pronounced than that for **3**–MTA-Au due to the relatively poor quenching effect of **2** or **4** by MTA-Au. Interestingly, the response sensitivity of the three sensors to LPS decreased remarkably as the affinity of fluorescent probes (**2–4**) to MTA-Au increased (Fig. 4), which indirectly reflects a competition of binding onto the surface of MTA-Au between LPS and fluorescent probes.

The selectivity of the three sensors for LPS determination was further evaluated and compared by their fluorescence responses to various biological important species (Fig. 5). We observed that biological species with multiple negative charges and hydrophobic groups/domains such as ssDNA (single-stranded DNA), dsDNA (double-stranded DNA), BSA (bovine serum albumin), and dNTP (deoxy-ribonucleoside triphosphate), induce a remarkable increase in fluorescence due to their strong cooperative non-covalent interactions with MTA-Au. Other small biological species do not lead to an obvious fluorescence response. It is noteworthy that the fluorescence response of **4**–MTA-Au to these biological species was significantly less sensitive as compared with that for the other two sensors, which led to a high selectivity to LPS. This has strong implications that the binding affinity of MTA-Au for LPS is significantly higher than that for other biological species, as a consequence that the fluorescent probe **4** bound on the surface of Au NPs can only be effectively replaced by the binding of LPS. This result, in combination with the preceding data, also indicates that the non-covalent binding strength between fluorescent probes and Au NPs has a significant influence on the sensitivity and selectivity of LPS sensing. However, to further increase the selectivity of LPS sensing without a compromise of the response sensitivity, more sophisticated surface engineering of Au NPs and more systematically optimizing the manner of synergy of non-covalent interactions between fluorescent probes and Au NPs are required.

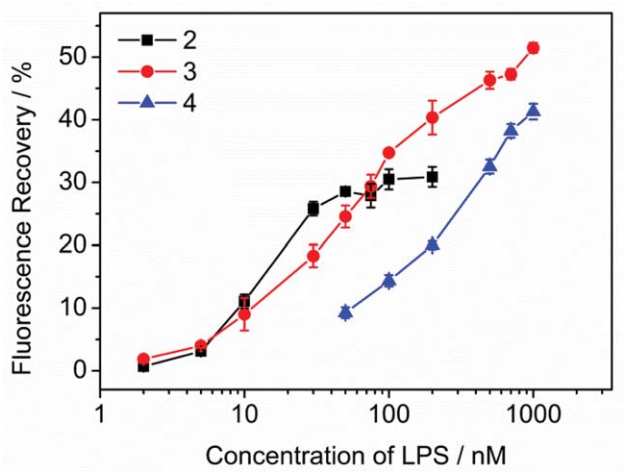

Fig. 4 Fluorescence recovery of probes (**2–4**) and MTA-Au supramolecular sensing systems in the presence of LPS in HEPES buffer (10 mM, pH 7.0, 20% ethanol). Data are presented as mean ± SD ($n = 3$).

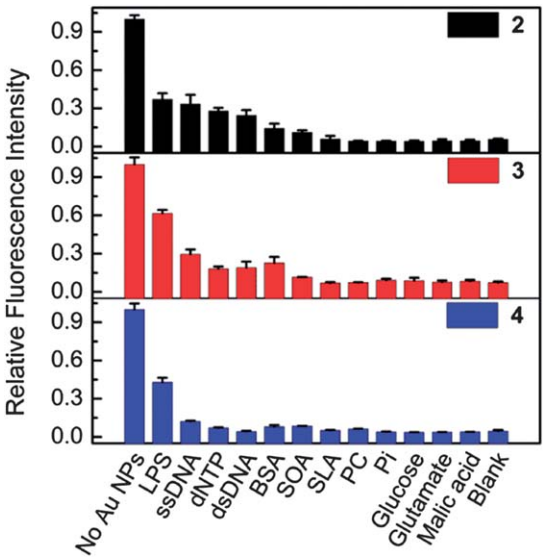

Fig. 5 Fluorescence response of **2–4** and MTA-Au supramolecular sensing systems to LPS and various biological important species in HEPES buffer (10 mM, pH 7.0, 20% ethanol); concentration of each species: ssDNA (single-stranded DNA), 1 μM; dNTP (deoxy-ribonucleoside triphosphate), 2 μM; dsDNA (double-stranded DNA), 2 mg L^{-1}; BSA (bovine serum albumin), 1 mg L^{-1}; SOA (sodium oleic acid), 2 μM; SLA (sodium lauric acid), 2 μM; PC (phosphatidylcholine), 2 μM; Pi (sodium phosphate), 2 μM; glucose, 2 μM; glutamate, 2 μM; malic acid, 2 μM; LPS, 0.5 μM in **2**–MTA-Au and **3**–MTA-Au systems; LPS, 1 μM in **4**–MTA-Au sensing system; no Au NPs refers to the fluorescence of **2–4**; blank refers to the fluorescence of **2–4** and MTA-Au assembled systems without the addition of any species. Data are presented as mean ± SD ($n = 3$).

Conclusions

In summary, the synergy of non-covalent interactions between fluorescent probes (*i.e.* guest molecules) and Au NPs has been systematically and quantitatively explored. We found that both the electrostatic attraction/repulsion and the hydrophobic interaction play very important roles to the binding of fluorescent

probes for Au NPs. Moreover, we demonstrated that a synergy of electrostatic attraction and hydrophobic stacking can not only lead to a very pronounced increase in the binding constant, but also allows the binding of fluorescent probes to the surface of Au NPs in a positively cooperative manner. Considering that the synergy of non-covalent interactions on the surface of nanoparticles is crucial for a broad range of applications, such an understanding is important. Finally, in light of the understanding of non-covalent interactions on the surface of Au NPs, hybrid systems that consist of Au NPs and surface-assembled fluorescent probes were exploited for fluorescent turn-on sensing of LPS. Our study shows that the sensitivity or selectivity to LPS relies strongly on the binding affinity between fluorescent probes and Au NPs. Comparing to other fluorescent turn-on sensors for LPS, fluorescent probes assembled Au NPs thus provide more straightforward and attractive alternatives for further optimization of sensitivity/selectivity of LPS sensing. New routes to increase the selectivity of LPS sensing without a compromise of its sensitivity could include the introduction of other interactions such as host–guest interactions and hydrogen bonds,[18] and the use of Au NPs with more sophisticated surface modifications. Thus, further development will also greatly benefit from the great number of Au NPs with diverse surface monolayers available in the literature.[19]

Acknowledgements

We would like to acknowledge the financial support of the National Natural Science Foundation of China (21075101), the National Basic Research Program of China (2011CB910403), Planned Science and Technology Project of Xiamen, China (3502z20113006), Specialized Research Fund for the Doctoral Program of Higher Education of China (200803840007), and NFFTBS (no. J1030415).

Notes and references

1 (*a*) L. S. Young, W. J. Martin, R. D. Meyer, R. J. Weinstein and E. T. Anderson, *Ann. Intern. Med.*, 1977, **86**, 456–471; (*b*) R. J. Ulevitch, *Adv. Immunol.*, 1993, **53**, 267–289; (*c*) R. J. Ulevitch and P. S. Tobias, *Curr. Opin. Immunol.*, 1994, **6**, 125–130; (*d*) G. H. Seltmann and O. Holst, *The Bacterial Cell Wall*, Springer, New York, 2002.

2 (*a*) C. R. Raetz, *Annu. Rev. Biochem.*, 1990, **59**, 129–170; (*b*) B. Beutler and E. T. Rietschel, *Nat. Rev. Immunol.*, 2003, **3**, 169–176; (*c*) E. S. Van Amersfoort, T. J. Van Berkel and J. Kuiper, *Clin. Microbiol. Rev.*, 2003, **16**, 379–414; (*d*) H. S. Warren, C. Fitting, E. Hoff, M. Adib-Conquy, L. Beasley-Topliffe, B. Tesini, X. Liang, C. Valentine, J. Hellman, D. Hayden and J-M. Cavaillon, *J. Infect. Dis.*, 2010, **201**, 223–232.

3 (*a*) P. F. Roslansky and T. J. Novitsky, *J. Clin. Microbiol.*, 1991, **29**, 2477–2483; (*b*) G.-H. Zhang, L. Baek, P. E. Nielsen, O. Buchardt and C. Koch, *J. Clin. Microbiol.*, 1994, **32**, 416–422.

4 (*a*) M. Rangin and A. Basu, *J. Am. Chem. Soc.*, 2004, **126**, 5038–5039; (*b*) S. Voss, R. Fischer, G. Jung, K.-H. Wiesmüller and R. Brock, *J. Am. Chem. Soc.*, 2007, **129**, 554–561; (*c*) V. Ganesh, K. Bodewits, S. J. Bartholdson, D. Natale, D. J. Campopiano and J. C. Mareque-Rivas, *Angew. Chem., Int. Ed.*, 2009, **48**, 356–360; (*d*) L. C. Henderson, J. Li, R. L. Nation, T. Velkov and F. M. Pfeffer, *Chem. Commun.*, 2010, **46**, 3197–3199; (*e*) L. Zeng, J. Wu, Q. Dai, W. Liu, P. Wang and C.-S. Lee, *Org. Lett.*, 2010, **12**, 4014–4017.

5 (*a*) J. Wu, A. Zawistowski, M. Ehrmann, T. Yi and C. Schmuck, *J. Am. Chem. Soc.*, 2011, **133**, 9720–9723; (*b*) M. Lan, J. Wu, W. Liu, W. Zhang, J. Ge, H. Zhang, J. Sun, W. Zhao and P. Wang, *J. Am. Chem. Soc.*, 2012, **134**, 6685–6694.

6 (*a*) G. Cooke and V. M. Rotello, *Chem. Soc. Rev.*, 2002, **31**, 275–286; (*b*) D. Bonifazi, S. Mohnani and A. Llanes-Pallas, *Chem.–Eur. J.*, 2009, **15**, 7004–7025; (*c*) A. Barnard and D. K. Smith, *Angew. Chem., Int. Ed.*, 2012, **51**, 6572–6581.

7 (*a*) M. Lundqvist, J. Stigler, G. Elia, I. Lynch, T. Cedervall and K. A. Dawson, *Proc. Natl. Acad. Sci. U. S. A.*, 2008, **105**, 14265–14270; (*b*) A. E. Nel, L. Mädler, D. Velegol, T. Xia, E. M. Hoek, P. Somasundaran, F. Klaessig, V. Castranova and M. Thompson, *Nat. Mater.*, 2009, **8**, 543–557; (*c*) X.-R. Xia, N. A. Monteiro-Riviere and J. E. Riviere, *Nat. Nanotechnol.*, 2010, **5**, 671–675.

8 (*a*) C.-C. You, O. R. Miranda, B. Gider, P. S. Ghosh, I.-B. Kim, B. Erdogan, S. A. Krovi, U. H. Bunz and V. M. Rotello, *Nat. Nanotechnol.*, 2007, **2**, 318–323; (*b*) C. K. Kim, P. Ghosh, C. Pagliuca, Z.-J. Zhu, S. Menichetti and V. M. Rotello, *J. Am. Chem. Soc.*, 2009, **131**, 1360–1361; (*c*) B. K. Gorityala, Z. Lu, M. L. Leow, J. Ma and X.-W. Liu, *J. Am. Chem. Soc.*, 2012, **134**, 15229–15232; (*d*) D. Zaramella, P. Scrimin and L. J. Prins, *J. Am. Chem. Soc.*, 2012, **134**, 8396–8399; (*e*) A. Bajaj, S. Rana, O. R. Miranda, J. C. Yawe, D. J. Jerry, U. H. F. Bunz and V. M. Rotello, *Chem. Sci.*, 2010, **1**, 134–138; (*f*) N. Pazos-Pérez, W. Ni, A. Schweikart, R. A. Alvarez-Puebla, A. Fery and L. M. Liz-Marzán, *Chem. Sci.*, 2010, **1**, 174–178.

9 D. F. Moyano, M. Goldsmith, D. J. Solfiell, D. Landesman-Milo, O. R. Miranda, D. Peer and V. M. Rotello, *J. Am. Chem. Soc.*, 2012, **134**, 3965–3967.

10 (*a*) H. Wei, B. Li, J. Li, E. Wang and S. Dong, *Chem. Commun.*, 2007, 3735–3737; (*b*) X. Xue, F. Wang and X. Liu, *J. Am. Chem. Soc.*, 2008, **130**, 3244–3245; (*c*) G. W. Doorley and C. K. Payne, *Chem. Commun.*, 2012, **48**, 2961–2963.

11 G. Frens, *Nat. Phys. Sci.*, 1973, **241**, 20–22.

12 S. K. Ghosh and T. Pal, *Chem. Rev.*, 2007, **107**, 4797–4862.

13 (*a*) D. Liu, W. Qu, W. Chen, W. Zhang, Z. Wang and X. Jiang, *Anal. Chem.*, 2010, **82**, 9606–9610; (*b*) D. A. Walker, C. E. Wilmer, B. Kowalczyk, K. J. Bishop and B. A. Grzybowski, *Nano Lett.*, 2010, **10**, 2275–2280.

14 H. Yuan, J. Miao, Y.-Z. Du, J. You, F.-Q. Hu and S. Zeng, *Int. J. Pharm.*, 2008, **348**, 137–145.

15 S. H. D. P. Lacerda, J. J. Park, C. Meuse, D. Pristinski, M. L. Becker, A. Karim and J. F. Douglas, *ACS Nano*, 2010, **4**, 365–379.

16 (*a*) B. Dubertret, M. Calame and A. J. Libchaber, *Nat. Biotechnol.*, 2001, **19**, 365–370; (*b*) Y.-W. Lin, C.-C. Huang and H.-T. Chang, *Analyst*, 2011, **136**, 863–871.

17 (*a*) C.-C. Huang and H.-T. Chang, *Anal. Chem.*, 2006, **78**, 8332–8338; (*b*) X. He, Z. Zhong, Y. Guo, J. Lv, J. Xu, M. Zhu, Y. Li, H. Liu, S. Wang, Y. Zhu and D. Zhu, *Langmuir*, 2007, **23**, 8815–8819; (*c*) T. I. Kim, J. Park and Y. Kim, *Chem.–Eur. J.*, 2011, **17**, 11978–11982.

18 (*a*) S. Mandal, A. Gole, N. Lala, R. Gonnade, V. Ganvir and M. Sastry, *Langmuir*, 2001, **17**, 6262–6268; (*b*) R. Baron, C. H. Huang, D. M. Bassani, A. Onopriyenko, M. Zayats and I. Willner, *Angew. Chem. Int. Ed.*, 2005, **44**, 4010–4015; (*c*) L. Du, S. Liao, H. A. Khatib, J. F. Stoddart and J. I. Zink, *J. Am. Chem. Soc.*, 2009, **131**, 15136–15142; (*d*) M. A. Olson, A. Coskun, R. Klajn, L. Fang, S. K. Dey, K. P. Browne, B. A. Grzybowski and J. F. Stoddart, *Nano Lett.*, 2009, **9**, 3185–3190; (*e*) X. Chen, S. G. Parker, G. Zou, W. Su and Q. Zhang, *ACS Nano*, 2010, **4**, 6387–6394.

19 (*a*) G. A. Devries, M. Brunnbauer, Y. Hu, A. M. Jackson, B. Long, B. T. Neltner, O. Uzun, B. H. Wunsch and F. Stellacci, *Science*, 2007, **315**, 358–361; (*b*) N. Vogel, M. Jung, N. L. Bocchio, M. Retsch, M. Kreiter and I. Köper, *Small*, 2010, **6**, 104–109; (*c*) D. M. Andala, S. H. R. Shin, H.-Y. Lee and K. J. M. Bishop, *ACS Nano*, 2012, **6**, 1044–1050; (*d*) H.-Y. Lee, S. H. R. Shin, L. L. Abezgauz, S. A. Lewis, A. M. Chirsan, D. D. Danino and K. J. M. Bishop, *J. Am. Chem. Soc.*, 2013, **135**, 5950–5953.

